Ocean and Sea Ice SAF

Technical Note
SAF/OSI/CDOP/KNMI/TEC/RP/143

Validation of SeaWinds 25 km winds

Anton Verhoef, Jur Vogelzang and Ad Stoffelen

Version 1.1

January 2008

DOCUMENTATION CHANGE RECORD

Reference: SAF/OSI/CDOP/KNMI/TEC/RP/143

Issue / Revision:	Date:	Change:	Description:
Version 1.0	Dec. 2007		First version.
Version 1.1	Jan. 2008	Minor	EUMETSAT comments taken into account

Contents

1. Introduction

This report is written to establish the quality of the EUMETSAT Ocean and Sea Ice Satellite Application Facility (OSI SAF) QuikSCAT wind fields, notably at high resolution (25 km). Currently, an operational OSI SAF QuikSCAT wind product is available at 100 km resolution. This product is especially suitable to assimilate into Numerical Weather Prediction models, but less appropriate for nowcasting, since small-scale phenomena in the wind fields are not visible. The 100-km product is made by spatially averaging the backscatter values that are available at 25 km resolution in the NOAA QuikSCAT product. This averaging is done in order to reduce the noise in the wind field. For the OSI SAF 25-km wind product appropriate meteorological structures are used to spatially smooth the noise. This is achieved by the combination of the so-called MSS and 2DVAR schemes as further elaborated below.

In the Multiple Solution Scheme (MSS), the wind solution ambiguities are not restricted to those corresponding two to four backscatter points of the Geophysical Model Function (GMF) that have minimum distance to the measurement point. These minimum distance points are determined by the backscatter measurement noise. Therefore, from high backscatter noise measurements, such as present in the 25-km WVCs, noisy wind solutions will emerge after the GMF inversion step. To solve this problem, in the MSS the full wind vector probability density function is kept represented by 144 ambiguities (rather than 2-4) with associated prior probabilities. Each ambiguity represents a 2.5° wind direction sector. The a priori probability of a wind ambiguity is proportional to its associated distance to the GMF in backscatter measurement space. All 144 wind solutions with their probabilities are input for the 2DVAR AR step. MSS is not used in the 100-km wind product, but it is shown in this report that the use of MSS is essential in order to get a 25-km wind field of good quality.

It has been shown that the Ambiguity Removal (AR) step in the wind processing reduces the noise in the wind product by spatially filtering the scatterometer wind solutions [*Portabella,* 2002]. Ambiguity Removal is the process of selecting the most probable wind solution out of an ambiguous wind solution set that is available after wind inversion in each Wind Vector Cell (WVC). Several AR schemes have been proposed [*Stoffelen,* 1998b; *Portabella,* 2002], and a number of schemes is implemented in the genscat library at KNMI, which lies at the base of the scatterometer processors for SeaWinds (SDP) and ASCAT (AWDP) that are developed within the Numerical Weather Prediction SAF. These AR methods have been compared and their results analysed [Stoffelen et al, 2000] on the basis of which a sophisticated 2-Dimensional Variational Ambiguity Removal (2DVAR) has been developed at KNMI.

The basic idea behind 2DVAR is to make a spatial analysis from the local WVC wind ambiguities and a weather model forecast following the methods discussed by *Daley* [1991], and to select the ambiguity closest to the analysis at each WVC. This requires knowledge on the error structure of both observations and weather model predictions. The advantage of 2DVAR over other schemes is that it explicitly uses the a priori probability information associated with the ambiguities.

Recently, the 2DVAR method has been critically reviewed. A number of bugs has been removed from the code and the underlying equations. The new 2DVAR is implemented in SDP from version 1.4 onwards. The current operational version of SDP is 1.5.

In principle, there are three ways for establishing the quality of the scatterometer wind fields:

- Comparison with buoy measurements or weather model winds
- Statistical analysis
- Case studies

This study is restricted to statistical analysis, weather model comparison and some case studies. On the basis of this it is possible to draw firm conclusions on the quality of the 25-km wind fields. Comparison of scatterometer wind products with independent buoy measurements is a proven method, especially when in addition weather model forecasts are considered within a triple collocation approach [*Stoffelen,* 1998a]. However, a large number of buoy data are needed over a period of one year in order to obtain good statistics. Buoy comparisons are planned for 2008.

In a statistical analysis the overall properties of the wind field are studied. In this report the following aspects are investigated:

1. Wind field comparison: analysis of the differences in terms of standard deviation between SDP wind fields on one hand and background wind fields generated by the National Centers for Environmental Prediction (NCEP) or the European Centre for Medium-range Weather Forecasts (ECMWF) on the other hand. See Chapter 3.

2. Noise level estimation: estimation of the amount of white noise in SDP wind fields using autocorrelation and spectral techniques. See Chapter 4.

A statistical assessment of the quality of the 25-km product is given in Chapter 5

In Weather Prediction one is particularly interested in extreme events: fronts, cyclones, and hurricanes. To prevent that such features become buried in the bulk of the data, case studies are needed to assess the quality of the scatterometer wind products. To this end, KNMI experimentally runs several versions of SDP in parallel routinely in order to detect problematic cases and test algorithmic improvements. See Chapter 6 for a selection of such cases.

Note that much of the contents of this report is extracted from a NWP SAF report [*Vogelzang,* 2007]. The NWP SAF report contains additional background information concerning 2DVAR, whereas this OSI SAF report focuses on the quality of the SeaWinds 25-km wind product. The AR step in combination with MSS is the key in obtaining good quality high-resolution winds and therefore this report is mainly devoted to aspects associated with this.

1.1. References

Chelton, D.B., M.H. Freilich, J.M. Sienkiewicz, and J.M. Von Ahn, 2006,
      On the use of QuikSCAT scatterometer measurements of surface winds for marine weather prediction. *Monthly Weather Review*, **134**, 2055-2071.

Daley, R., 1991,
      Atmospheric Data Analysis.
      Cambridge University Press, Cambridge, New York, USA.

Portabella, M., 2002,
      Wind retrieval from satellite radar systems.
      Thesis, University of Barcelona, Barcelona, Spain.

Press, W.H., B.P. Flannery, S.A. Teukolsky, and W.T. Vetterling, 1987,
      Numerical Recipes.
      Cambridge University Press, Cambridge, UK.

OSI SAF team KNMI, 2008,
      SeaWinds Product Manual.
      Available through www.osi-saf.org and www.knmi.nl/scatterometer/publications/

Stoffelen, A., 1998a,
      Toward the true near-surface wind speed: Error modeling and calibration using triple collocation.
      Journal of Geophysical Research, 1103 C4, 7755-7766.

Stoffelen, A.C.M., 1998b,
      Scatterometry.
      Thesis. Universiteit Utrecht, Utrecht, The Netherlands.

Stoffelen, A., S. de Haan, Y. Quilfen and H. Schyberg,
      ERS Scatterometer Ambiguity Removal Scheme Comparison
      Document external project: 2000, OSI SAF, EUMETSAT.
      www.knmi.nl/publications/fulltexts/safosi_w_arcomparison.pdf

Vogelzang, J., 2006,
      On the quality of high resolution wind fields
      Report NWPSAF-KN-TR-002, UKMO, UK.
      www.metoffice.gov.uk/research/interproj/nwpsaf/scatterometer/index.html

Vogelzang, J., 2007,
> Validation of 2DVAR on SeaWinds data
> Report NWPSAF-KN-TR-005, UKMO, UK.
> www.metoffice.gov.uk/research/interproj/nwpsaf/scatterometer/index.html

1.2. Abbreviations and acronyms

2DVAR	Two Dimensional Variational Ambiguity Removal
AR	Ambiguity Removal
ASCAT	Advanced SCATterometer
AWDP	ASCAT Wind Data Processor
BUFR	Binary Universal Form for the Representation of meteorological data
ECMWF	European Centre for Medium-Range Weather Forecasts
EUMETSAT	European Organisation for the Exploitation of Meteorological Satellites
GMF	Geophysical Model Function
KNMI	Royal Netherlands Meteorological Institute
MSS	Multiple Solution Scheme
NCEP	National Centers for Environmental Prediction
NOAA	National Oceanic and Atmospheric Administration
NWP	Numerical Weather Prediction
OSI	Ocean and Sea Ice
SAF	Satellite Application Facility
SDP	SeaWinds Data Processor
VQC	Variational Quality Control
WVC	Wind Vector Cell

2. Data and processing

All SeaWinds data from December 2004 were evaluated for this study. The data set contained all orbits that started in this period, orbits 28388 up to and including 28829. The NOAA BUFR files were processed with SDP 1.5 using either the NCEP model wind field (which is provided in the NOAA BUFR product) or the ECMWF wind field as background. The NCEP model wind field is a 24 hour forecast of the 1000 mb winds. The ECMWF wind field is a 3 – 9 hour forecast of the wind speeds at 10 m anemometer height, and is therefore expected to compare better with the scatterometer winds (which are also at 10 m).

After processing, the data of each orbit is contained in a separate BUFR output file. The length of some of the BUFR output files turned out to depend on which background field was used, ECMWF or NCEP, due to incompleteness of the input BUFR data. There were eight such files, listed in table 3.1. They were disregarded for further analysis. The remaining processed data set consists of 434 full orbits.

Orbit	Date
28412	02 Dec
28432	04 Dec
28500	08 Dec
28501	08 Dec
28547	12 Dec
28548	12 Dec
28623	17 Dec
28738	25 Dec

Table 1   Orbits in the December 2004 dataset excluded from further analysis

As SeaWinds is a rotating fan beam scatterometer, its observation geometry varies along the swath. At 25 km resolution there are 76 WVCs, and the swath is divided in three parts: the outer swath (WVC 1-10 and 67-76), the mid swath or "sweet" swath (WVC 11-30 and 47-66), and the nadir swath (WVC 31-46). See also table 2.

Swath name	WVC range	Main properties
outer	1-10 and 67-76	Less than 4 σ_0 observations and therefore not processed by SDP
mid or "sweet"	11-30 and 47-66	Good observation geometry
nadir	31-46	Bad observation geometry: σ_0 observations almost 180° separated and therefore noisy results

Table 2   SeaWinds swath properties at 25 km resolution

During all runs there was only one batch (with 18 WVCs) for which 2DVAR could not find a solution for the minimisation problem. In such a case 2DVAR returns the closest-to-background solution. This single batch will not affect the results presented here.

3. Wind field comparison

The datasets described in the previous section were inter-compared by calculating the statistics of the differences between the zonal components, u, and the meridional components, v. Tables 3a and 3b show the standard deviations of the differences in zonal wind component, σ_u, and meridional wind component, σ_v, respectively. The tables are, of course, symmetric. Only the upper right parts have been calculated, the lower left parts have been filled in to facilitate searching. Weather model wind vectors were only considered if the associated scatterometer wind vectors (no-MSS or MSS) were valid. This is done to prevent the NCEP and ECMWF model wind vectors to be contaminated by land pixels in the comparison.

The largest differences occur between the no-MSS wind and the NCEP model ($\sigma_u \approx 2.5$ m/s; $\sigma_v \approx 2.2$ m/s). It makes little difference whether the selected winds were obtained using the NCEP winds or the ECMWF winds as background, indicating the independence of the product on the background wind. Note that the differences between the no-MSS winds and the ECMWF model ($\sigma_u \approx 1.9$ m/s; $\sigma_v \approx 1.8$ m/s) are smaller than those between the no-MSS winds and the NCEP model ($\sigma_u \approx 2.5$ m/s; $\sigma_v \approx 2.2$ m/s). This means that the scatterometer winds are closer to the ECMWF model than to the NCEP model. As the ECMWF first guess wind is better than the NCEP + 24 hour 1000 mb wind, it is concluded that the scatterometer observations yield useful information.

σ_u (m/s)		NCEP			ECMWF		
		Model	no-MSS	MSS	Model	no-MSS	MSS
NCEP	Model	--	2.53	2.14	1.79	2.54	2.22
	no-MSS	2.53	--	1.21	1.93	0.59	1.27
	MSS	2.14	1.21	--	1.52	1.29	0.60
ECMWF	Model	1.79	1.93	1.52	--	1.94	1.48
	no-MSS	2.54	0.59	1.29	1.94	--	1.22
	MSS	2.22	1.27	0.60	1.48	1.22	--

Table 3a   Standard deviation of the differences in the zonal wind component.

σ_v (m/s)		NCEP			ECMWF		
		Model	no-MSS	MSS	Model	no-MSS	MSS
NCEP	Model	--	2.22	1.95	1.75	2.22	2.07
	no-MSS	2.22	--	1.06	1.76	0.43	1.09
	MSS	1.95	1.06	--	1.50	1.08	0.55
ECMWF	Model	1.75	1.76	1.50	--	1.75	1.41
	no-MSS	2.22	0.43	1.08	1.75	--	1.06
	MSS	2.07	1.09	0.55	1.41	1.06	--

Table 3b   Standard deviation of the differences in the meridional wind component.

This is confirmed by the results for the MSS winds. Now the 2DVAR method has more freedom in selecting the optimal wind vector, and the influence of the background field becomes more important. The difference between the MSS wind field and the NCEP model is rather large when using the ECMWF winds as background ($\sigma_u \approx 2.2$ m/s; $\sigma_v \approx 2.1$ m/s) and somewhat smaller when using the NCEP wind as background ($\sigma_u \approx 2.1$ m/s; $\sigma_v \approx 2.0$ m/s). Compared to the ECMWF winds, the differences are smaller: $\sigma_u \approx \sigma_v \approx 1.5$ m/s with NCEP background; $\sigma_u \approx 1.5$ m/s and $\sigma_v \approx 1.4$ m/s with ECMWF background, denoting only a small effect of the ECMWF background in the validation.

This is consistent with the notion that without MSS the ambiguity removal method has limited choice between the (four at most) solutions found by the inversion algorithm, and therefore the details of the background field are less important. However, note that the difference between the MSS winds obtained with either NCEP background or ECMWF background is

similarly small ($\sigma_u \approx 0.60$ m/s; $\sigma_v \approx 0.55$ m/s), i.e., the effect of the background field is small as compared to the other 2DVAR inputs (scatterometer wind pdf and spatial filtering constraints).

Applying MSS to the NCEP background reduces the standard deviation of the error with respect to the ECMWF model with $\sqrt{(1.79)^2 - (1.52)^2} = 0.95$ m/s for u and with $\sqrt{(1.75)^2 - (1.50)^2} = 0.90$ m/s for v. This again shows the added value of scatterometer information derived with MSS on the scales described by the ECMWF model. Note that the no-MSS winds based on the NCEP wind field actually add variance to the ECMWF-NCEP difference, thereby degrading the wind field.

The results in tables 3a and 3b were obtained for those wind vectors for which the Variational Quality Control flag was not set. The number of valid vectors may therefore differ slightly for each of the sets. Table 4 shows the number of wind vectors involved. The number of points varies between 18.8 million and 19.2 million, a variation of 2%. Such a variation may have influence on the statistics.

N ($\times 10^6$)		NCEP			ECMWF		
		Model	no-MSS	MSS	Model	no-MSS	MSS
NCEP	Model	--	18.9	18.9	18.8	18.8	18.8
	no-MSS	18.9	--	19.2	18.9	18.8	18.8
	MSS	18.9	19.2	--	18.8	18.8	19.0
ECMWF	Model	18.8	18.9	18.8	--	19.2	19.2
	no-MSS	18.8	18.8	18.8	19.2	--	19.2
	MSS	18.8	18.8	19.0	19.2	19.2	--

Table 4   Number of points in the intercomparisons.

However, as shown in tables 5a and 5b, the absolute deviation, i.e., the average of the absolute value of the difference, is smaller than the standard deviation in all cases. This indicates that the distributions of the differences are sharply peaked, without significant outliers. The ratio of the standard deviation to the absolute deviation ranges from 1.3 to 2.2. Only for the difference between the selected solutions without MSS the ratio is around 10, indicating very sharp peaked, almost delta function-like distributions.

a_u (m/s)		NCEP			ECMWF		
		Model	no-MSS	MSS	Model	no-MSS	MSS
NCEP	Model	--	1.95	1.67	1.38	1.96	1.74
	no-MSS	1.95	--	0.76	1.41	0.06	0.76
	MSS	1.67	0.76	--	1.17	0.78	0.27
ECMWF	Model	1.38	1.41	1.17	--	1.42	1.14
	no-MSS	1.96	0.06	0.78	1.42	--	0.77
	MSS	1.74	0.76	0.27	1.14	0.77	--

Table 5a   Absolute deviation of the differences in the zonal wind component.

a_v (m/s)		NCEP			ECMWF		
		Model	no-MSS	MSS	Model	no-MSS	MSS
NCEP	Model	--	1.68	1.45	1.33	1.68	1.50
	no-MSSI	1.68	--	0.70	1.34	0.04	0.71
	MSS	1.45	0.70	--	1.15	0.70	0.26
ECMWF	Model	1.33	1.34	1.15	--	1.34	1.12
	no-MSS	1.68	0.04	0.70	1.34	--	0.70
	MSS	1.50	0.71	0.26	1.12	0.70	--

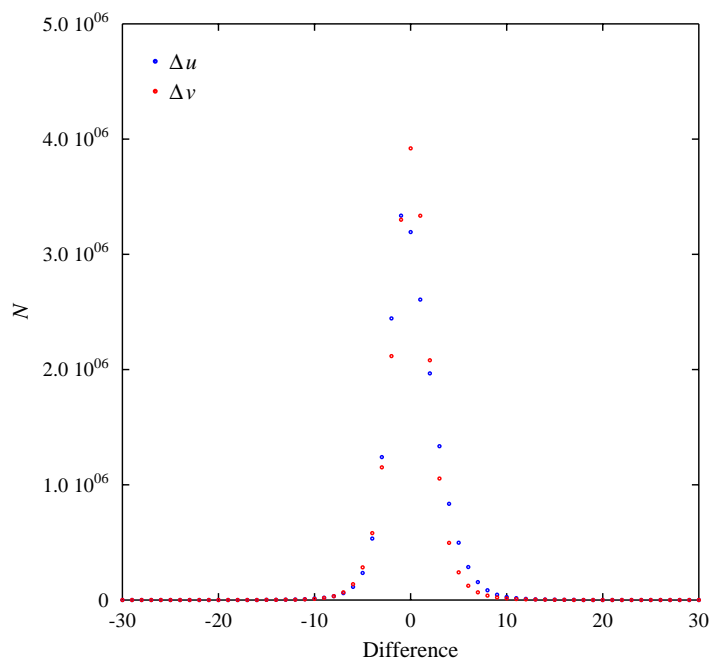**Table 5b**   Absolute deviation of the differences in the meridional wind component.

Figure 1 Histogram of the differences between the NCEP model field and the scatterometer field with ECMWF as background. No MSS has been applied.

As an example, figure 1 shows the histogram for the difference between the NCEP model and the selected solution with ECMWF background and without MSS. The other histograms are similar.

We conclude on the scales as represented by the ECMWF model that

- The scatterometer adds relevant information;

- The background used in 2DVAR has a statistically small contribution in both the MSS and the non-MSS modes, though smallest for non-MSS;

- MSS clearly contributes to improve the quality of the wind field.

4. Small scales and noise level

The wind field comparisons in section 3 imply verification with the spatial scales as represented by the ECMWF model. However, the scatterometer provides information on yet smaller scales. In this section we evaluate the statistical and spectral properties on these smaller scales of the OSI SAF scatterometer products processed at KNMI. In addition, we study the random wind fluctuations (error) of these products.

It is well known that wind fields obtained from SeaWinds backscatter data at 25 km resolution often have a noisy appearance, especially in the nadir part of the swath. There are several ways to estimate the noise content. The most widely used method is to estimate the noise variance from the spectrum which is the absolute square of the Fourier transform of the autocorrelation function (see, e.g., *Press et al.* [1987]). White noise shows up as a constant contribution to the spectrum.

Figure 2 shows the spectrum of the zonal and meridional wind components u and v at 25 km resolution from the ECMWF model and from SDP with and without MSS using the ECMWF winds as background. As a reference, the dashed black line shows a k^{-2} spectrum. The spectra for the SDP wind components without MSS (dashed red and blue curves) indeed tend to become horizontal at high frequencies, indicating the presence of noise, but also the other curves slightly bend here.
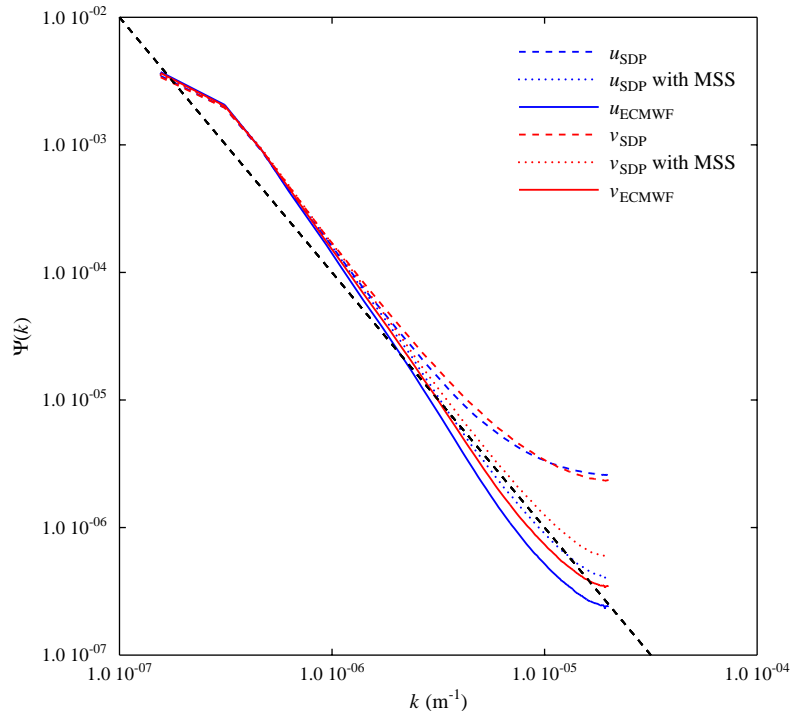
Figure 2 Spectra of the zonal and meridional wind components u and v at 25 km resolution from the ECMWF model and from SDP with and without MSS. The dashed black curve is for a k^{-2} spectrum.

It has been shown by *Vogelzang* [2006] that this is due to numerical effects in the FFT algorithm used to calculate the spectrum. These effects, in turn, are caused by the fact that the autocorrelation function does not fall off to zero fast enough. As a matter of fact, the autocorrelation will never fall off to zero because for example the trade winds will cause correlation over long distances. It is hard to separate these sampling effects from noise.

Figure 2 shows that SDP wind fields contain more small-scale information than the ECMWF fields. The SDP results with MSS (which are free of noise as will be shown later in this chapter) contain 15% more signal at scales of 1000 km ($k = 10^{-6}$ m^{-1}) than the ECMWF winds. At scales of 100 km ($k = 10^{-5}$ m^{-1}) the difference has increased to almost 75%, which means a

factor 3 in the wind energy. At this point it should be noted that *Chelton et al.* [2006] find a much steeper fall off for the model wind spectra. The reason for this difference is most probably due to handling of the data and calculation of the spectra, but the details are not clear yet.

A better way to estimate the noise level is to analyse the autocorrelation itself. A white noise component adds variance but no correlation, so it expresses in the autocorrelation function as a delta-function peak at zero distance.
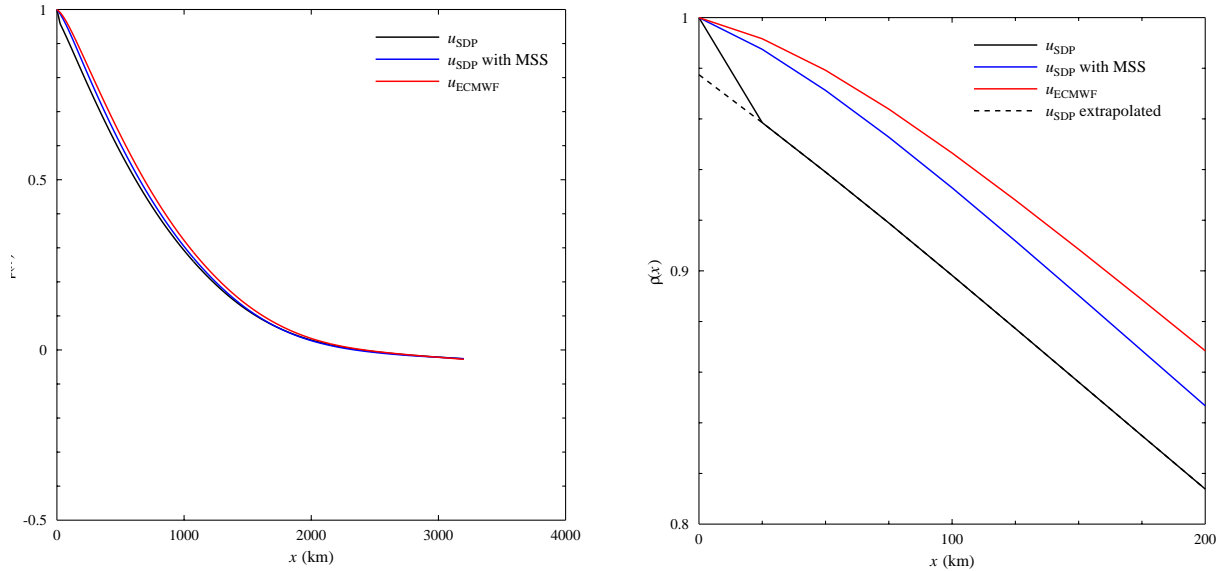
Figure 3   Autocorrelation of the zonal wind component *u* from the ECMWF model and from SDP with and without MSS.

Figure 3 shows the autocorrelation in the zonal wind component *u* at 25 km resolution obtained from the ECMWF field and from the SDP results with and without MSS. The left hand panel shows the full curves; the right hand panel shows an enlargement at short distances. The SDP result without MSS (black curve) shows a clear discontinuity at short distances, while the SDP result with MSS (blue curve) and the ECMWF result (red curve) approach 1 continuously at short distances. Note that the MSS and the no-MSS curves run largely parallel denoting that the correlated wind structures, which are presumably meteorological, are kept by 2DVAR MSS. Moreover, the autocorrelations show that ECMWF winds fall off slower, indicating less small-scale information in line with the conclusion on figure 2.

The size of the discontinuity can be estimated by extrapolating the curve to zero distance (dashed black curve). It is directly related to the white noise variance. The results are shown in figure 4 for the SDP wind components at 25 km and 50 km resolution. The estimated white noise variances have been converted to standard deviations. At coarser resolutions the white noise level clearly reduces. Note that as the extrapolation distance increases, larger uncertainties in the noise estimate occur. The extrapolation may even somewhat overshoot the autocorrelation, leading to an extrapolated autocorrelation larger than 1 at *x=0* and, hence, a negative white noise variance estimate. This happens at 50 km resolution in the mid swath and at 100 km resolution all over the swath. These points have been excluded from figure 4.
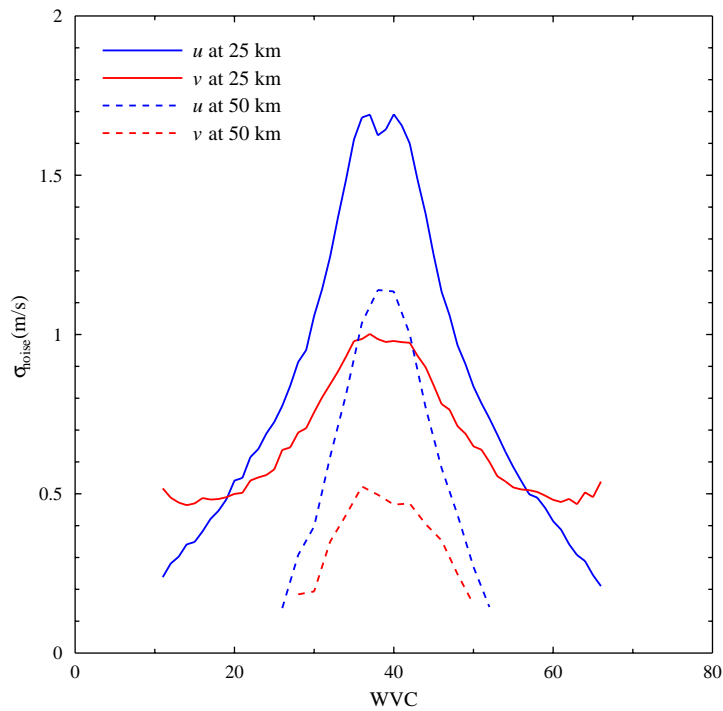
Figure 4   Standard deviation of the white noise in the zonal and meridional wind components u and v obtained by SDP at 25 km and 50 km resolution.

Figure 4 shows that the noise level decreases as the resolution becomes coarser. At 100 km resolution the noise estimates are invalid. This is interpreted as indicating negligible noise contribution, see the discussion above. At 25 km resolution the standard deviation of the noise may exceed 1 m/s for *v* and 1.5 m/s for *u*. Note that these figures are somewhat higher than reported earlier by *Vogelzang* [2006]. The reason for this difference is that the new noise levels are obtained with SDP1.5 which deviates more from the background than results with SDP1.3. Therefore, in SDP1.3 results the background has more influence, while SDP1.5 results mainly show the observations, leading to higher noise levels without MSS.

When MSS is applied the noise component disappears in line with figure 3 (no results shown).

5. Accuracy of the 25-km product

Figure 5 shows two-dimensional histograms of the OSI SAF-retrieved 25-km winds versus ECMWF forecasts. The data are from consecutive orbits from 1-5 July 2007.
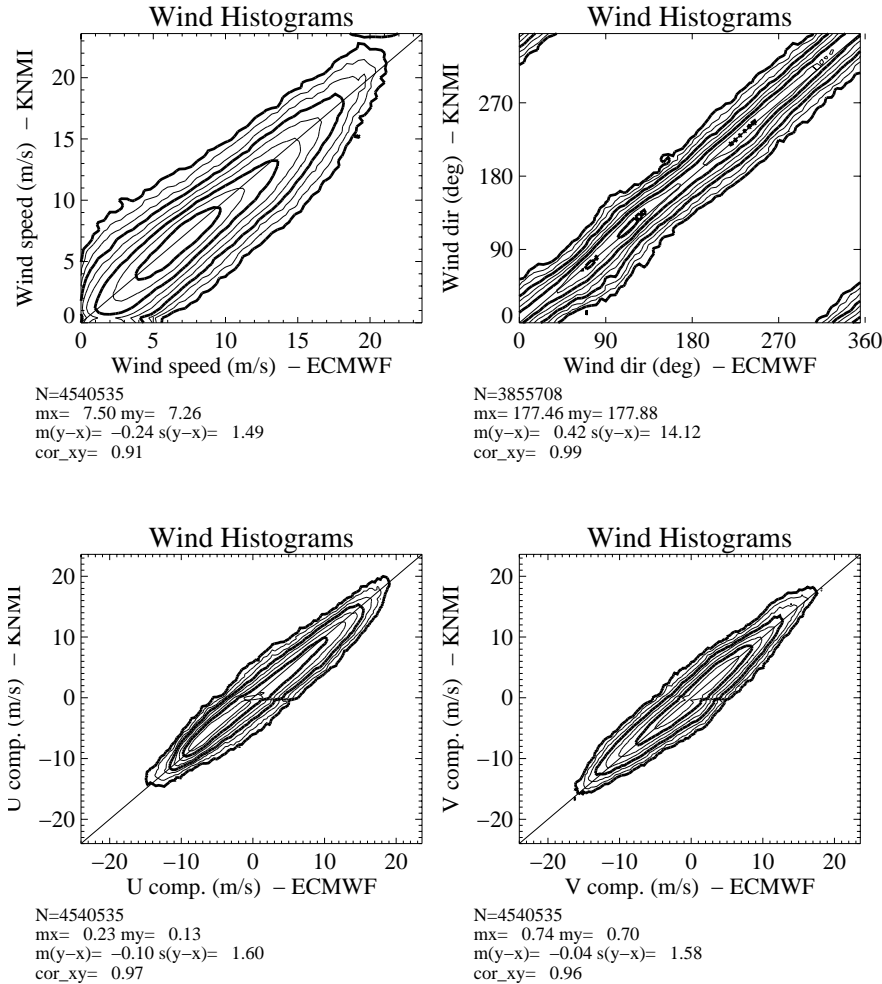
Figure 5 Contoured histograms of the 25-km KNMI wind product

The top left plot corresponds to wind speed (bins of 0.4 m/s) and the top right plot to wind directions (bins of 2.5°). The latter are computed for ECMWF winds larger than 4 m/s. The bottom plots show the *u* and *v* wind component statistics. N is the number of data; mx and my are the mean values along the x and y axis, respectively; m(y-x) and s(y-x) are the bias and the standard deviation with respect to the diagonal, respectively; and cor_xy is the correlation value between the x- and y-axis distributions. The contour lines are in logarithmic scale: each step is a factor of 2 and the lowest level (outer-most contour line) is at N/64000 data points.

From these results, it is clear that the spread in the distributions is small. The wind speed bias is quite small and it is clear from the bottom plots that the standard deviations in the components are well below 2 m/s.

6. Cases

Two cases are shown to illustrate the typical effects of MSS and 2DVAR in the 25-km products. Although the superior ECMWF background is used in the operational processing, here two cases are provided using the NCEP 1000-mb wind as background in 2DVAR. In this way, the beneficial impact of the observations can be more clearly shown and a fair comparison can be made to DIRTH winds from NOAA at 25 km resolution that also are produced with the NCEP 1000-mb winds as background.

6.1. South China Sea

Figure 6 shows the NOAA results for the SeaWinds wind field in the South China Sea recorded on January 18, 2004 (orbit 37050-37051). As can be seen from figure 6, the DIRTH ambiguity removal scheme yields a rather noisy wind field, notably around 5° north. In some WVCs the rain flag is set. These cells are shown as an orange arrow.
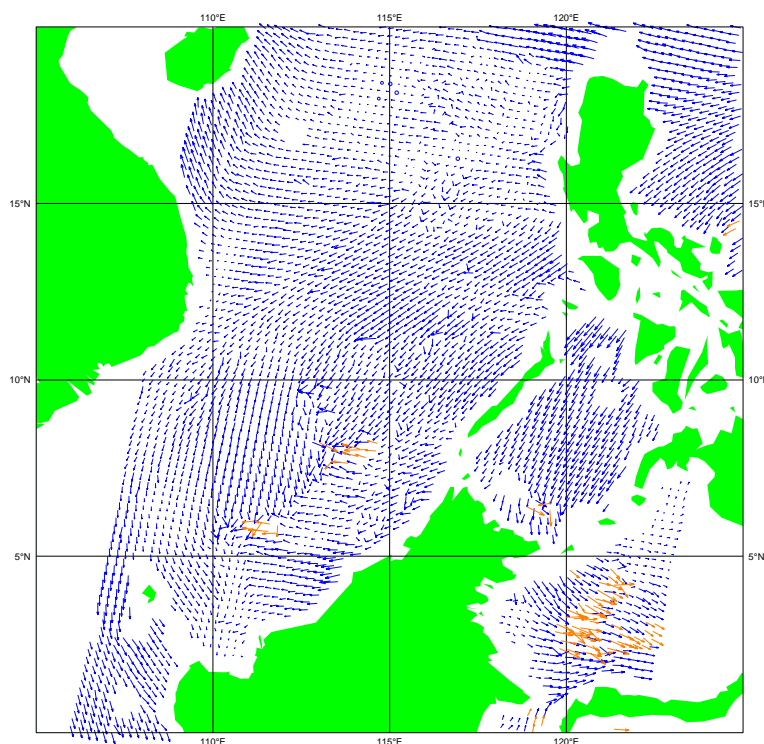
Figure 6   NOAA wind field over the South China Sea at January 18, 2004. The orange arrows indicate cells for which the JPL rain flag has been set.

Figure 7 shows the NCEP background field corresponding to figure 6. The background field is perfectly smooth. Figure 8 shows the SDP wind field without applying the MSS and using the NCEP field as background. The resulting wind field is rather noisy, especially at nadir. The NOAA rain flag is deactivated during SDP processing. Note that for only a few WVCs around 8° N, the Variational Quality Control flag is set (indicated with a purple arrow). Cells with the MLE flag set are rejected by SDP at 25 km resolution. The MLE flag is a combination of the NOAA rain flag and KNMI's quality control procedure based on the MLE.
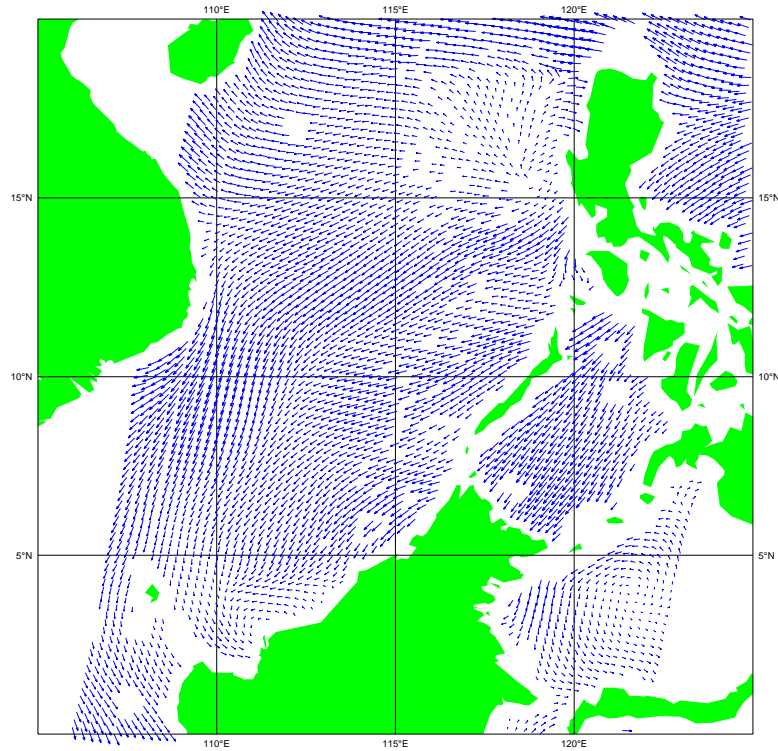
Figure 7   NCEP model field for South China Sea at January 18, 2004.
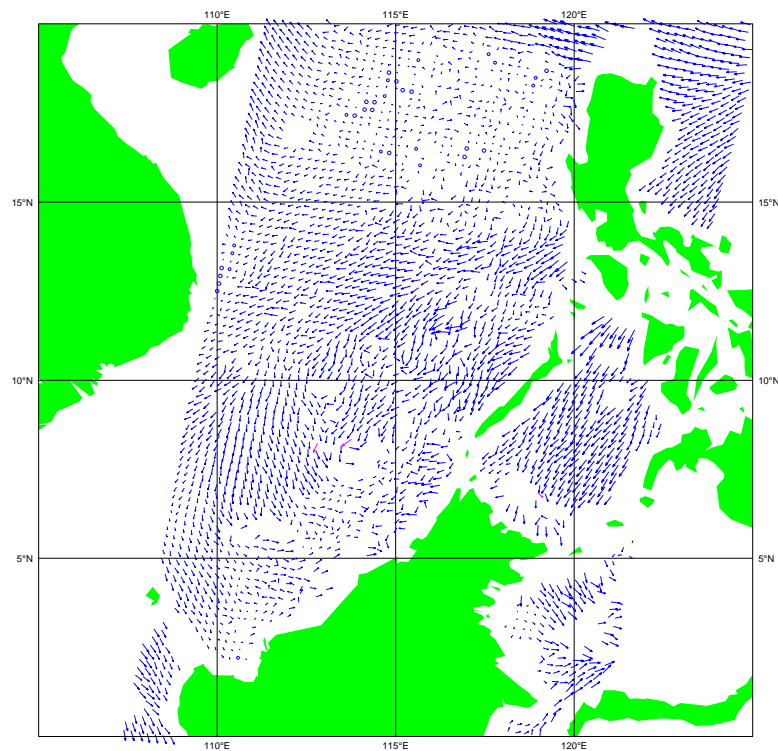

Figure 8   SDP result for the South China Sea wind field on January 18, 2004. No MSS has been applied.
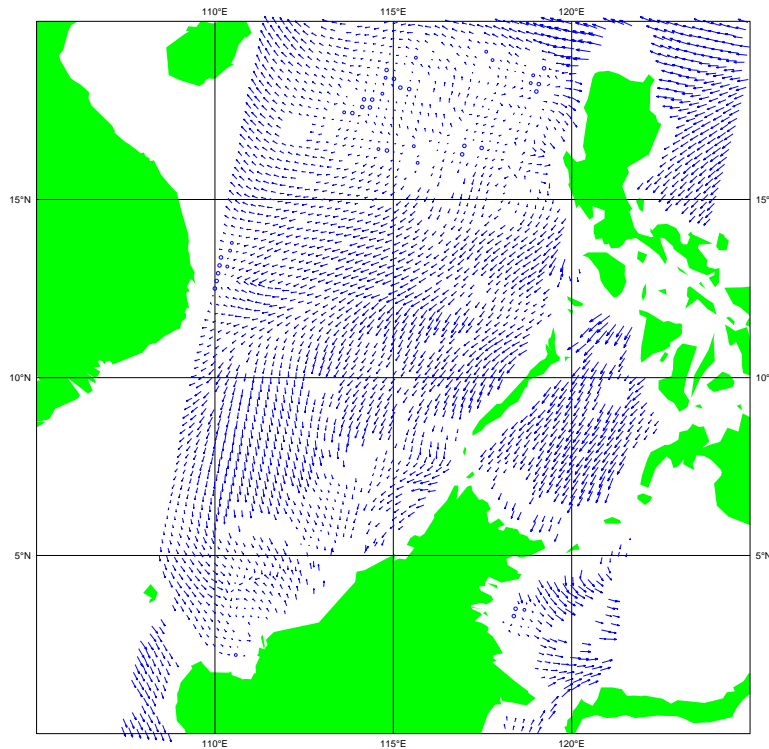
Figure 9 SDP with MSS.

The noise can be removed by applying the MSS, as shown in figure 9. Moreover, the VQC quality control detects no false solutions. Note that the scatterometer winds are weaker than the NCEP 1000 mb model wind as expected, especially in the western part of the area between the Philippines and the Asian main land.

Note the different circulation pattern in the low wind area (115° - 120° E; 15° - 20° N). Though the wind field produced by 2DVAR with MSS (figure 9) is much smoother than that without MSS (figure 8), it differs much from the background NCEP field (figure 7). The MSS wind field contains a small vortex in the middle of the low wind area. This vortex is below the resolution of the NCEP model. There are also some inconsistent winds near the northwestern coast of Kalimantan.

6.2. Pacific front

Figure 10 shows the NOAA result for SeaWinds measurements recorded on August 6, 2006 in the Pacific Ocean off the coast of Chile. A strong low pressure area located approximately at 80° W and 45° S is accompanied with an extended frontal area on its northern and northeastern side. The front has an irregular shape right of the middle of figure 10 where a large number of cells have their rain flag set (orange arrows). To the north of the front a few erroneous wind vectors can be seen.

This shape is not present in the NCEP model field shown in figure 11. Moreover, the NCEP model locates the front more to the south (the grid point 80° W, 30° S is a suitable reference), and the centre of the low pressure area more to the west.

The SDP wind field without MSS is shown in figure 12. The wind field is noisy and the southeastern part of the front is not very clearly visible because many points there are rejected from processing by SDP.
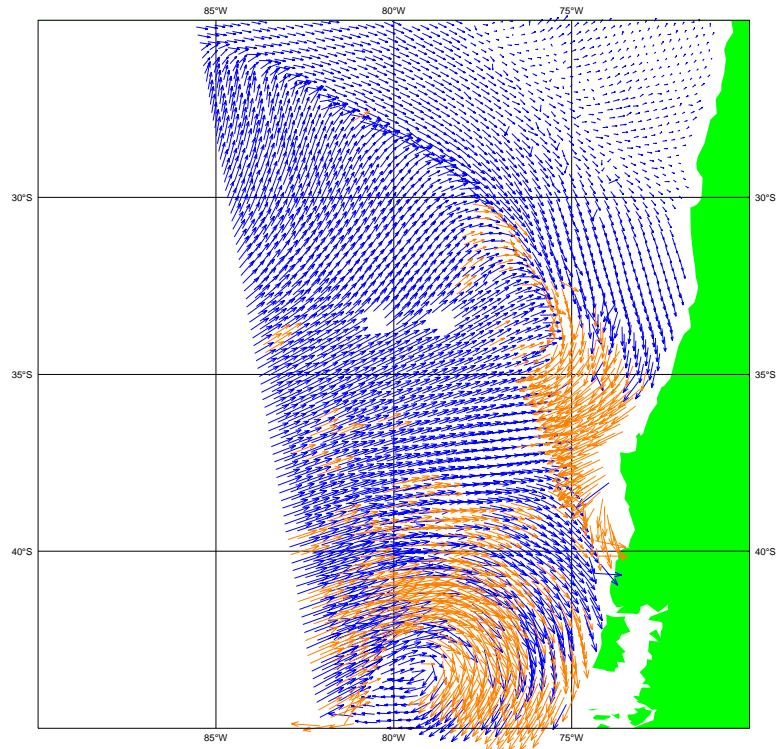
Figure 10   NOAA wind field over the Pacific Ocean at August 6, 2006. The orange arrows indicate
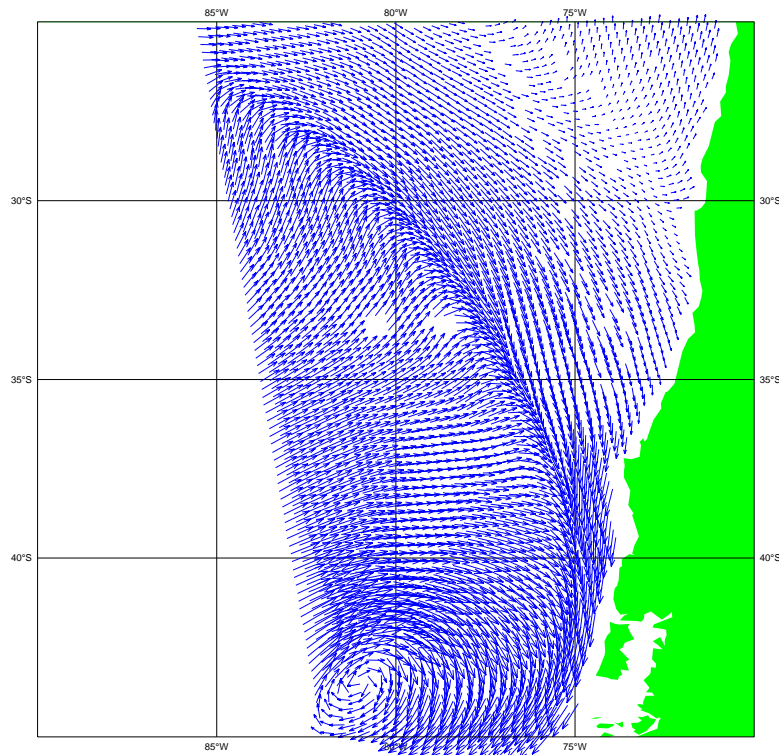WVCs for which the JPL rain flag is set.
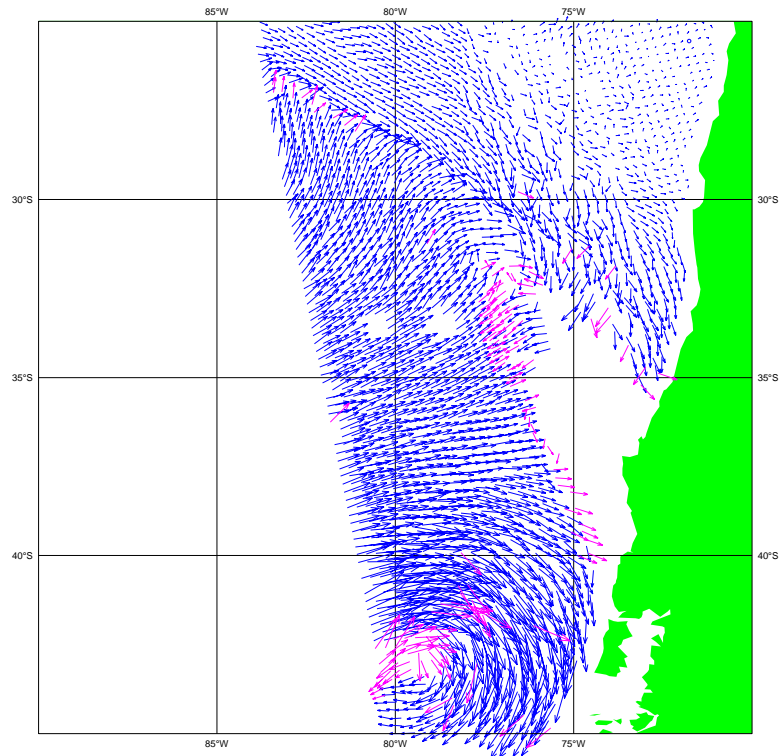

Figure 11   NCEP model field.
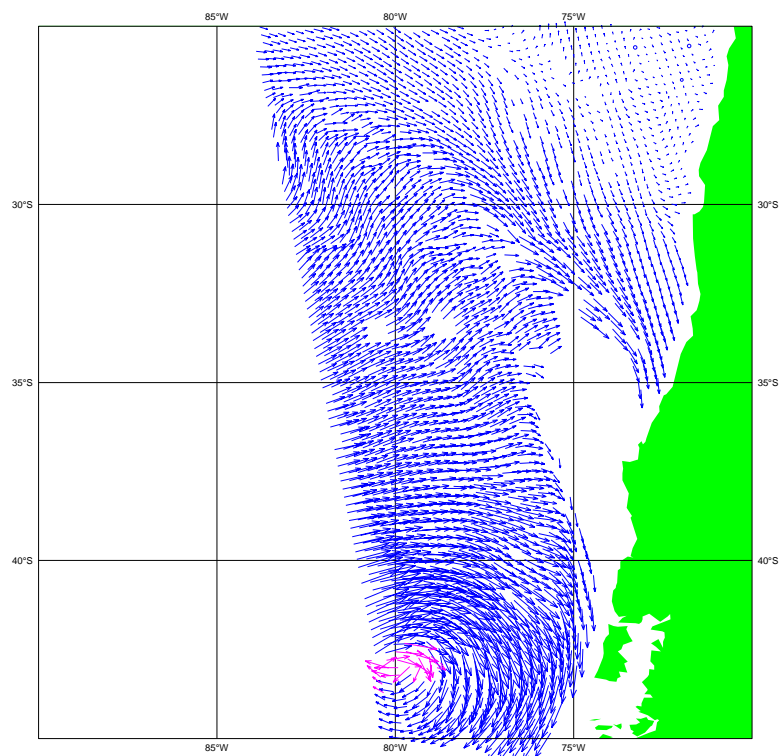
Figure 12   SDP without MSS.

Figure 13   SDP with MSS.

The Variational Quality Control (VQC) flag is set in a number of WVCs along the front and near the centre of the low pressure area (purple arrows), but less WVCs are flagged than in

figure 10. The location of the centre of the low pressure area agrees with the NOAA result, figure 10, while the location of the front agrees with the NCEP background, figure 11. Note the strong convergence in the region 30°S - 35°S, 75°W - 80°W. This structure seems not realistic.

Figure 13 shows the result when MSS is applied. The wind field is smooth, also north of the front. The front appears smoother and extends more to the southeast. No WVCs are flagged in the frontal zone. Southwest of the front line some wavy structures appear in the wind field. The convergence in the region 30°S - 35°S, 75°W - 80°W has disappeared, and the centre of the low pressure area has moved slightly to the west.

The case studies show that 2DVAR is influenced stronger by the background field with MSS than without. This effect is particularly apparent in cases where observations and background differ, for example in the position of a front or a cyclone. It is caused by the fact that MSS retains 144 ambiguities, so 2DVAR has much more chance of finding an ambiguity with reasonable a priori probability close to the background than in the traditional scheme with 4 solutions at most. However, MSS is needed to filter out the white noise component in the SeaWinds data at 25 km resolution, so the increased influence of the background can be regarded upon as the price to be paid: too less background influence may destroy 2DVAR's noise filtering properties. The effect of the background may be diminished by further fine tuning its error model: increasing the error standard deviation or decreasing the correlation length, see also [*Vogelzang,* 2007].

Large discrepancies between observations and background as in the case of the Pacific front relatively seldom occur - about once or twice per month on average. One should therefore be careful with changes in the current values of the parameters in the 2DVAR error model

7. Conclusions

From the statistical analyses and the case studies in the previous chapters the following picture emerges for 25-km SeaWinds wind fields processed with SDP:

Processed without MSS at 25 km resolution, the SDP wind fields contain a substantial noise component with a standard deviation that varies with WVC number. The standard deviation of the noise in the nadir swath is up to 1.1 m/s for the meridional component v and 1.7 m/s for the zonal component u.

This study shows that wind fields at 25 km resolution obtained from SeaWinds data and processed by SDP with MSS and 2DVAR are accurate and reliable. Details in the wind field appear that are neither discernable in the background model winds nor in the wind fields obtained without MSS.

2DVAR with MSS effectively removes the white noise, while it retains most of the small-scale meteorological information. The wind field verification with and without MSS indicates an average improvement of 0.9 m/s in the standard deviation of the difference between the SDP wind field and the ECMWF model prediction when applying MSS. This number, which is an average over all WVCs, is consistent with the white noise standard deviation obtained from the autocorrelation analysis.

In a few cases the 25-km SeaWinds product is shown to depend on the background wind field used in 2D-VAR. This is particularly apparent in cases where observations and background give different positions for features like fronts or cyclones. As these cases are rather rare, more investigations over an extended period are needed to decide if further fine tuning of the 2DVAR error model is necessary.

At 25 km resolution SDP needs the MSS in order to remove the noise contained in the SeaWinds data, notably in the nadir part of the swath. At 50 km still noise is present in the nadir swath. At coarser resolution, notably 100 km, the spatial backscatter averaging reduces the noise and the effect of MSS disappears. These results validate a posteriori the OSI SAF 100-km product without MSS.

Although the current 25-km product has a clear additional value to the existing SeaWinds products, further analysis and validation by a triple collocation of 25-km, 100-km SeaWinds and buoy wind data is recommended for the future.